Shape-Controlled Colloidal Synthesis of Rock-Salt Lead Selenide Nanocrystals

Ali M. Jawaid, Daniel J. Asunskis,[†] and Preston T. Snee[*]

Department of Chemistry, University of Illinois at Chicago, 845 West Taylor Steet, Chicago, Illinois 60607-7061, United States [†]Present address: Department of Science, Black Hills State University, 1200 University Street, Spearfish, South Dakota 57799.

ABSTRACT Developing simple synthetic methods to control the size and morphology of nanocrystals is an active area of research as these parameters control the material's electronic and optical properties. For a semiconductor with a symmetrical crystal structure such as lead selenide, anisotropic colloidal growth has been previously accomplished *via* the use of templates, seeds, or by block assembly of smaller, symmetrical subunits. Here, we present a simple method to create monodisperse lead selenide nanorods and multipods at low temperatures. The size distribution and the observed morphologies are consistent with a continuous, anisotropic growth of material. The syntheses of these anisotropic shapes are due to the nature of the nuclei that form upon injection of precursors into partially oxidized alkene solvents that may contain lactone and carbonate-functional derivatives.

KEYWORDS: nanocrystals · lead selenide · shape-controlled nanocrystals · quantum confinement · nanorods

Research on colloidal semiconductor nanocrystals has garnered much attention due to the material's excellent photostability, size dependent optical and electronic properties, and their promising use in biological imaging and sensing applications.[1−3] Several physical attributes are tunable by controlling both the size and shape of the nanomaterials;[4,5] for example, polarized emission in quantum confined systems has been observed in nanorods with aspect ratios greater than 2.[6] Electrical and magnetic properties may also be manipulated with shape control. This can lead to exciting new areas for the implementation of these anisotropic systems. The unique electronic and optical properties of rod-shaped nanocrystals (NCs)[7−9] have made it possible to create NC semiconductor lasers which have much lower gain thresholds.[10,11] Furthermore, "nanobarbells" composed of a semiconductor rod bound by metal "bells" create the possibility of wiring the structures for conductivity measurements; these materials also show great potential as photocatalysts.[12−14] Rod-shaped NCs also have utility as the active element in solar cells.[15−17] A very recent, transformative result has demonstrated that a semiconductor dot-core coated by a rod-shaped shell, with a metal deposited[18] selectively at one end, is a very promising material for the photocatalytic generation of hydrogen.[19] The sum of these results demonstrate that shape control of semiconductor NCs has generated a wealth of scientific breakthroughs in the nanoscience community.

Semiconducting lead chalcogenides are ideal materials to study because of their large Bohr exciton radii which allow easy access to the strongly confined regime. In the case of lead selenide, the bulk band gap (0.27 eV) can be tailored to overlap in the telecommunication broadband range[20] by size tuning particles using established colloidal nanocrystal synthesis schemes.[21] The observation of anisotropic shapes of lead selenide nanomaterials is especially of interest as its highly symmetrical rock salt crystal lattice would ostensibly make the existence of an anisotropic growth mechanism impossible. Previous studies circumvented this issue to create shape-controlled lead chalcogenide nanostructures by heterogeneous seeding,[22−24] ion exchange of templates,[25] chelation of precursors,[26] and directed NC monomer assembly.[27−30] Each of these mechanisms has their advantages and disadvantages; in a seeded growth system, for example, the heterogeneous catalyst used to unidirectionally grow nanorods may also alter the innate electronic and optical properties of the material.[31,32] Cation exchange affords great control over morphology but it is overall a complex process. Furthermore, unidirectional growth through multidentate ligands or monomer stacking does not afford morphological control over small length scales.

We report several low-temperature, one step syntheses of lead selenide NCs that

* Address correspondence to sneep@uic.edu.

Received for review May 6, 2011 and accepted July 19, 2011.

Published online July 19, 2011
10.1021/nn2016716

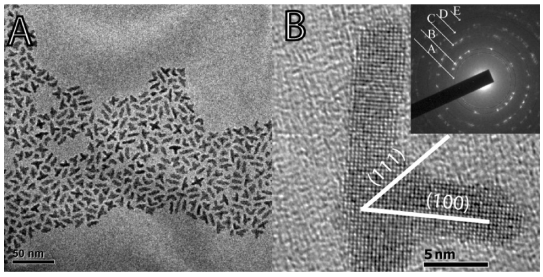

Figure 1. (A) Low-resolution transmission electron micrograph of PbSe nanorods and branched rods prepared by method B; (B) HRTEM micrograph of left. Inset: selected area diffraction pattern shows agreement with PbSe lattice planes (A, 111; B, 200; C, 220; D, 222; E, 322).

directly form rods and multipods (dipods, tripods, tetrapods, and pentapods). The method was discovered due to the inadvertent oxidation of the polyunsaturated solvent (squalene) that affords the production of anisotropic PbSe NCs. While the absolute identity of this species has remained elusive, we demonstrate how the functional moieties identified (lactone and/or cyclic carbonate) afford asymmetric morphologies.

RESULTS AND DISCUSSION

Our initial studies on PbSe NC synthesis were focused on the effects of surface chemistry on the nanocrystals' nonlinear optical properties.[33] During this work, anisotropic nanorods and "T"-shaped nanocrystals were occasionally formed ($\sim^1/_4$ of the preparations) using a procedure with an unsaturated squalene solvent and a lead acetate trihydrate precursor (method A). Figure 1 shows representative distributions of nanorods and branched structures we have synthesized from this method. As can be seen, the dominant rod morphology produced appears at a 3:2 ratio with "T"-shaped tripodal PbSe NCs. Analysis of 200 of the rod-shaped PbSe NCs reveals a 4.7 $\pm$ 0.5 nm width and an average length of 13.4 $\pm$ 1.9 nm yielding an aspect ratio of 2.8 $\pm$ 0.5. The minority tripodal NCs have a width of 4.4 $\pm$ 0.5 nm with long and short rod lengths of 14.3 $\pm$ 1.8 and 9.3 $\pm$ 1.0 nm, respectively. High resolution transmission electron microscopy (HRTEM) analysis confirms that the synthesized rods are high quality single crystals as shown in Figure 1B. Varying the reaction conditions, discussed below, yields several types of other anisotropic nanocrystals.

We noted that in these preparations (method A), the squalene solvent became slightly discolored during the initial degassing step. No discoloration was observed when using a fully saturated squalane solvent (method B); furthermore, the use of squalane does not afford the formation of anisotropic NCs. We reasoned that the chemical species that imparts the discoloration was responsible for the formation of short PbSe rods and "T"-shaped nanocrystals in the squalene solvent. This byproduct likely forms *via* the oxidation of the solvent by the water and acetic acid (*via* substitution

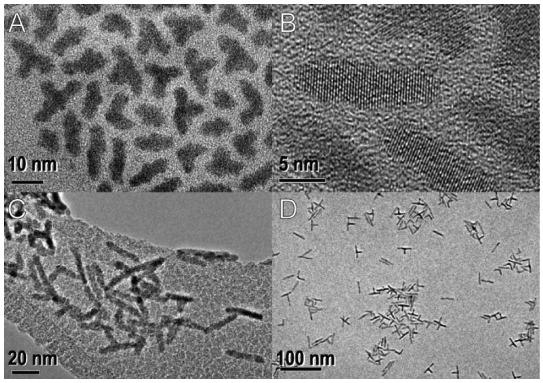

Figure 2. (A) PbSe NCs synthesized in squalene. (B) HRTEM of micrograph of sample A, aspect ratio = 2.8. (C) Squalene treated once with 2 mmol acetic acid and 3 mmol water, aspect ratio = 4. (D) Squalene treated thrice with 2 mmol acetic acid and 3 mmol water, aspect ratio = 7.

on a double bond) that is present due to the use of a lead acetate trihydrate precursor. To address this issue in a more controlled fashion, squalene was treated with acetic acid and water directly to identify the source of the solvent discoloration and to determine its role in PbSe NC synthesis.

Figure 2 illustrates the effect of treating squalene with water and acetic acid on the morphology of the PbSe NC products that form using methods A and C. As discussed previously, the use of squalene that was only exposed to the lead acetate trihydrate precursor did not reproducibly produce nanorods; more often, *ca.* 3−4 nm spherical particles were observed. Anisotropic PbSe NCs were consistently created when squalene was intentionally oxidized with water and acetic acid (method C); furthermore, greater solvent treatment resulted in nanomaterials with increasing aspect ratios. This effect appears to saturate after three treatments of the solvent with water and acetic acid resulting in nanorods with aspect ratios of 7 $\pm$ 2. Prolonged heating of the squalene mixture, in excess of 3 h, did not affect the morphologies of the synthesized nanoparticles. Furthermore, the use of a squalene solvent treated with extra water and acetic acid affords the formation of a wide variety of multipods as shown in Figure 3. Treatment with trifluoroacetic acid and water affords only dot and rod-shaped nanomaterials as shown in Figure S1 of the Supporting Information (SI); this result shows that control over the multiple morphologies is possible.

Analysis of Oxidized Squalene. Previous reports have shown that squalene and similar unsaturated hydrocarbons can undergo a wide variety of oxidation reactions including polyepoxidation and hydroxylation,[34] and lactone cyclization.[35] GC−MS analysis of the acetic acid-treated squalene was inconclusive and revealed multiple products as trace impurities (~0.3% by mass, SI, Figure S2). Of all these products, only one was identified as an oxidized derivative of squalene (SI,

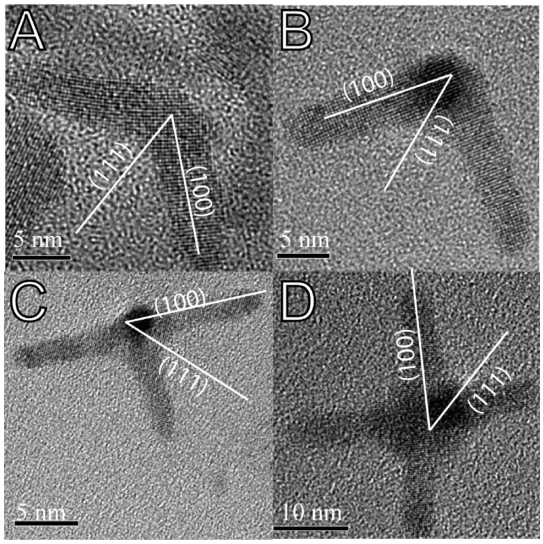

Figure 3. HRTEM micrograph of a variety of multipods synthesized by method C in a single reaction.

Figure S2, inset); however, we were not able to characterize any of these byproducts further. To aid in the analysis, the solvent was treated with a much stronger acid. As discussed in method D, squalene was mixed with trifluoroacetic acid and water in a sealed round-bottom flask under N_2; this resulted in the formation of a dark yellow-orange colored solution at room temperature. A mass spectral analysis confirms multiple products (SI, Figure S3); as such, we did not perform further GC−MS analysis. Fortunately, an FTIR study of the sample (SI, Figure S4) revealed a characteristic carbonyl peak at 1779 cm^{-1} and two additional features at 1219 and 1167 cm^{-1}. After careful review of a database of IR spectra of organic compounds,[36] this spectrum is consistent with either lactone or cyclic carbonate functional organic materials. ^{13}C and ^{1}H NMR revealed a ^{13}C peak at 156 ppm that is consistent with cyclic carbonates and is supported with ^{1}H NMR resonances at ~4.7 ppm (SI, Figure S4).[36] These data suggest that there may be multiple-substituted products formed that contain the same functionality; this accounts for well-defined FTIR and NMR spectra.

To investigate if lactones and cyclic carbonates can affect the morphologies of PbSe nanocrystals, γ-nonanoic lactone or propylene carbonate was used in lieu of TFA treated squalene in the synthesis of PbSe NCs (method E). The system was extremely sensitive to the concentration of γ-nonanoic lactone; as such, the reaction conditions had to be adjusted to observe some of the morphologies produced by methods B and C. At low loading ratios of γ-nonanoic lactone (0.1% by mass) the reaction did afford the formation of multipods and spherically symmetric particles; however, these results were poorly reproducible. We attributed this to the lactone boiling off (bp ≈ 125 °C) prior to TOPSe injection. At higher loading ratios (1% → 5% by solvent mass), the as-prepared materials frequently precipitated within minutes after precursor injection. Samples that did not were analyzed to reveal the formation of mostly dot- and rod-shaped PbSe NCs (SI, Figure S8). Electron microscopy analysis of the spherically symmetric particles reveal the presence of both (100) and (111) crystallographic facets that may allow for the anisotropy to form as discussed below. When γ-nonanoic lactone was introduced after TOPSe injection, as detailed in method F, the reaction failed to produce multipodal species as shown in Figure S9 of the SI. This indicates that γ-nonanoic lactone alters the PbSe nuclei in such a way as to allow the formation of anisotropic NCs. The addition of propylene carbonate, 20% by volume, also afforded asymmetric PbSe NC morphologies (SI, Figure S8,D).

Mechanism of Formation. Previous studies on wurtzite cadmium chalcogenide semiconductor NCs demonstrated that anisotropic growth is a consequence of the existence of a unique crystal axis; as such, similar growth mechanisms cannot be employed to create novel morphologies in rock-salt structured PbSe NCs due to the equivalencies of all (100) crystal facets. While we have elucidated the chemical origins of forming PbSe anisotropic nanoparticles, the physical mechanism for creating these structures were also investigated. Anisotropic PbSe shapes can arise from discrete directed monomer assembly (*i.e.*, oriented attachment), the formation of multifacted nuclei, or may arise from the continuous growth *via* a catalytic nanoparticle "seed" produced *in situ*.[22−24] If a fortuitous "seed" nanoparticle is present, it would most likely be composed of metallic lead or lead oxide formed during oxidation of squalene. We have ruled out a seeded growth mechanism for the anisotropy based on selected area electron diffraction (SAED) patterns and X-ray photoelectron spectroscopy (XPS) results. It has been shown previously that metal seeded substrates or otherwise alloyed substrates emerge as diffraction rings in SAED data.[24] Even after thorough washing of the template particle, SAED often resolves one or more atomic plane through Bragg diffraction of a crystal face (Figure 1B inset). Only PbSe lattice planes are visible, without evidence for metallic Pb or PbO lattices, indicative of a nodule where the onset of growth would occur. Although the (222) plane for PbSe and (220) plane for metallic Pb overlap, and these rings are seen in the diffraction pattern, this is not conclusive evidence for the presence of Pb^0 as the simple cubic face of metallic lead is not observed. XPS data (SI, Figure S10) demonstrate minimal oxidation of the PbSe particles and confirm that the lead is present in the +2 oxidation state; as such, there is little evidence to suggest elemental lead or lead oxide is present and directing the growth of anisotropic PbSe nanocrystals.

Additionally, it is possible for mixed faceted magic-sized clusters (MSC) to be produced *in situ*, and growth could be afforded by elongation on (100) crystallographic

planes while suppressed on (111) planes. However, we have performed experiments in which MSC were injected with the TOPSe into the reaction solution and only minimal asymmetry is observed (bullet shaped) and mostly spherically symmetric particles are present (SI, Figure S11). This suggests that formation of magic sized clusters is not sufficient in itself to produce the asymmetry we observe in our reactions.

Oriented attachment is a mechanism that is often employed to explain the formation of rod and wire shaped semiconductor nanostructures from dipolar NC building-blocks. Electrostatically polarized PbSe NCs can be created by the presence of high energy Pb or Se terminated (111) facets on the corners of the underlying cubic structure.[29] In such cases, two classes of surface structures emerge: six (100) nonpolar facets, and eight (111) Pb or Se polar terminated facets. Through this mechanism, PbSe NC monomers may become polarized with the right combination of "edge" (111) facets that facilitates monomer unidirectional oligomerization to form extended rod and wire structures.[29] Initially, we believed that our observations of short rod and "T"-shaped crystalline NCs were due to the same mechanism; the formation of small, polarized PbSe NCs that conjoin together over a small length scale. However, close examination of low and high resolution transmission electron microscopy images of these samples began to cast doubt on this assumption. Given that ~11% of monomer PbSe NCs with (111) facets should lack polarity, these species should be observable in electron microscopy studies. No such PbSe NC monomers were observed in any growth solution or precipitated sample. We also examined aliquots of the solution (method C) over time to investigate the preformation of nanorods and possibly to isolate nuclei prior to anisotropic growth. As shown in Figure S12 of the SI, rod and multipodal PbSe NCs are formed 90 s after TOPSe injection; at no point are small spherical or cubic monomers resolved. As no such species are observed, it is unlikely that anisotropic PbSe NCs are formed *via* oriented attachment.

The observations of a ~15% monodispersity in the length of the PbSe rods prepared by our method is also inconsistent with the lack of size control of the oriented attachment mechanism as the polarity is maintained throughout growth and would have no preferential bias to terminate. Additionally, we would expect integer aspect ratios for the as-synthesized materials due to the overall cubic symmetry of the monomers.[28] While our measurements are very close to whole number ratios (and in fact are within error), a closer examination of the statistical distribution of widths and lengths for the rod samples demonstrate that the length of the rod PbSe nanocrystals is decoupled from their widths.

A statistical analysis of the morphology of the nanorods shown in Figure 2D was performed to determine whether our observations are due to oriented attachment of polarized monomers. A sample of 288 rods was analyzed to calculate the statistical distribution of their lengths and widths. The first interesting observation concerns the sharpness of the width distribution as shown in Figure 4; these data are best fit to a Gaussian line shape. We next assessed the possibility that the distributions of the widths and length are related which would be the case of rods formed by oriented attachment.[28] As the aspect ratio of the rods is very close to 7, we calculated a large set of rod lengths by adding seven random numbers that conform to the width distribution; this Monte Carlo set of rod lengths was analyzed using the same statistical methods as the experimental data. As shown in Figure 4, our Monte Carlo analysis relating the width to the length distributions does not mimic the observed data ($R^2 = -1.6$ *vs* 0.98 for a best Gaussian fit); further, inclusion of other whole number aspect ratios does not improve the result suggesting the electrostatic assembly of multiple particles is not producing the PbSe nanorods. These data show that there are two separate growth mechanisms present because the two nanorod profiles (width and length) do not correlate to each other. A similar statistical analysis of the smaller aspect ratio rods synthesized by method A also leads to the same conclusion as shown in Figure S13 of the SI. Different mechanisms are therefore responsible for the initial particle nucleation and a subsequent growth into nanorod and branched rods on the (100) axis.

Nucleation-Controlled Morphology. As we have ruled out the formation of anisotropic PbSe NCs *via* previously observed processes and have demonstrated that our observations are chemical in origin, we believe that these rod and multipod shaped PbSe nanocrystals are created *via* a nucleation-controlled mechanism similar to that reported by the Cheon group for PbS NCs.[37] At the low temperature regime, nuclei can form containing both (100) and (111) facets; the (111) facets persist during growth as the low temperature does not allow for the NC to anneal into a fully cubic structure. Further, electron microscopy examinations of small particles that form in the presence of γ-nonanoic lactone show that they have mixed (100) and (111) faceting. The presence of organic ligands with a preferential association for one facet over the other allows for competitive growth from two different crystallographic axes forming rods and multipods. Because our samples contained many cubically arranged multipodal structures, the proposed squalene-derived lactone and/or cyclic carbonate functional species must preferentially interact with the nominally higher-energy (111) facets to lower its chemical potential such that growth in this direction is stunted. Elongation on the (100) planes would then afford the creation of the multipodal species present in the syntheses; this also is confirmed by TEM analysis which shows that the long axis is

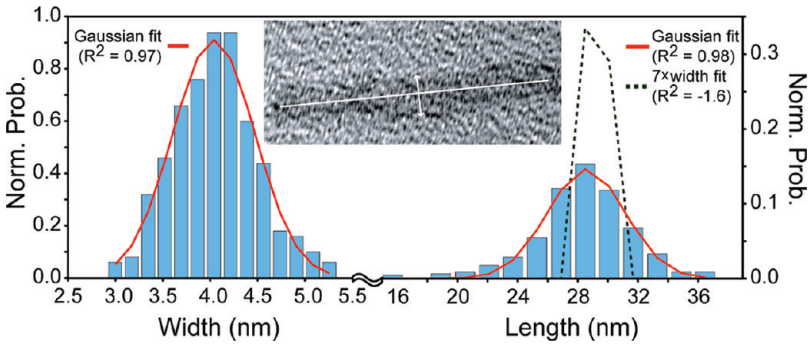

Figure 4. (Left) Distribution (blue bar) and fit (red) for PbSe nanorod widths. (Right) Distribution (blue bar) and Gaussian fit (red) for PbSe nanorod lengths. Dotted green: distribution predicted *via* oriented attachment mechanism.

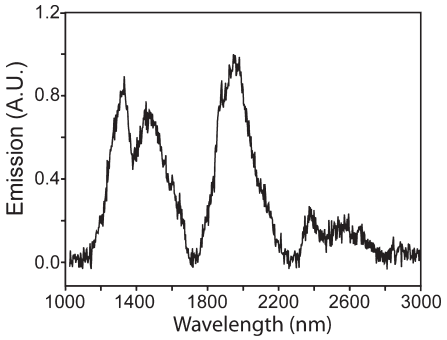

Figure 5. Photoluminescence spectra representative of a typical sample produced with method C. The multiple emission features are attributed to the presence of several multipods synthesized simultaneously in the oxidized squalene solvent.

always in the (100) direction. Some phenomenological models of multipodal seeds are shown in SI, Figure S14.

Optical Properties. The anisotropic PbSe NCs we have developed have several interesting optical properties. As shown in Figure 5, multiple emissive species are produced by method C as shown in the photoluminescence scan from 1000→3000 nm. We attribute this to the formation of a large number of multipodal structures; as shown in Figure S15 of the SI, only two features are observed with the rod and "T"-shaped NCs produced by method A. The fairly extreme range of the emission profile may be due to the low effective masses of the charge carriers (<0.1 m_e) and the large excitonic Bohr radius (46 nm) in PbSe.[38] If the most red-shifted feature originates from pentapodal NCs and the higher energy ~1300 nm emitters are rods, this demonstrates that quantum confinement in PbSe is significantly sensitive to the shape of the NCs. Essentially, the wavefuctions of the light charge carriers are diffuse enough to "bend" around the corners of the multipods to lower the kinetic confinement energy; we are investigating these properties further to make definitive assignments. It is also interesting to note that our samples have retained their emissive properties for months despite storage under "bench-top" conditions; this is a significant find as lead selenide nanoparticles are known to be prone to oxidation and quenching.[39] Overall, these results demonstrate that the emissive properties of anisotropic lead selenide NCs are greatly enhanced.

CONCLUSION

We have developed a novel method for synthesizing high quality nanorods and multipods of lead selenide. Control of the aspect ratios and dominant morphology has been demonstrated to be a function of solvent oxidation. These anisotropic shaped NCs were not produced *via* oriented attachment or by a catalytic nanoparticle seed formed *in situ*; furthermore, statistical analyses of rod-shaped structures indicate that nucleation and anisotropic growth are decoupled. Our results have shown that oxidation of the squalene solvent creates a lactone or cyclic carbonate functional species that directs the nucleation of PbSe NCs into structures with mixed (111) and (100) faceting. The (111) facets are likely passivated by these organic ligands such that growth only occurs in the (100) direction as previously observed in anisotropic PbS NCs. This conclusion is confirmed by the fact that the intentional addition of a lactone or carbonate also affords the formation of anisotropic PbSe NCs. We hope these results facilitate investigation into more complex nanostructures and nanodevices for lead selenide, especially as the emissive properties of anisotropic PbSe NCs are significantly more robust than dot-shaped materials.

MATERIALS AND METHODS

Lead acetate trihydrate ($Pb(ac)_2$, 99.98%), oleic acid (>99%), acetic acid (glacial, 99.8%), trifluoroacetic acid (TFA, 99%), γ-nonanoic lactone (97%), were purchased from Sigma-Aldrich. Squalane and squalene were purchased from Acros. Selenium shot (99.999%) and trioctylphosphine (TOP, 97%) were purchased from Strem. Propylene carbonate (99%), anhydrous hexane, and ethanol were purchased from Alfa-Aesar. All

chemicals were used without further purification unless noted. A 1 M trioctylphosphine selenide (TOPSe) solution was synthesized by mixing TOP and Se shot overnight; the solution was stored in an inert-atmosphere glovebox. Holey carbon TEM grids were purchased from SPI.

TEM measurements were performed on a JEOL JEM-3010F electron microscope. Emission data was taken on a custom-made Horiba Jobin Yvon fluorolog-3 spectrofluorometer with a short-arc xenon lamp at an excitation of 500 nm. FTIR was taken on a Genesis Matson FTIR. Gas chromatography mass spectrometry (GC–MS) analysis was performed on a JEOL GCMate II. X-ray photoelectron spectroscopy (XPS) analysis was carried out on all samples using a VSW HA-150 hemispherical analyzer with monochromatic X-radiation from an Al Kα source. The spectra were all calibrated to the C 1s in the hydrocarbon surfactant (oleic acid) at 285 eV; charge neutralization was not needed for this analysis. NMR spectra were measured with a Bruker Avance-400 spectrometer. All data were analyzed with Matlab.

Method A. Synthesis of PbSe Multipods in Squalene. A solution of 4 mL of squalene, 1 mL of TOP, 3 mmol oleic acid, and 1 mmol $Pb(ac)_2$ was dried under vacuum at 110 °C for 1 h in a 3-neck round-bottom flask. The resultant solution acquired a slight yellow discoloration. This solution was quickly heated to 125–135 °C under moderate N_2 flow, and 2 mL of a 1:1 mixture of 1 M TOPSe/TOP was rapidly injected. The temperature remained constant, and the particles were grown for 5 min. The product was precipitated in hexane with the addition of ethanol.

Method B. Synthesis of PbSe Nanoparticles in Squalane. A solution of 4 mL of squalane, 1 mL of TOP, 3 mmol oleic acid, and 1 mmol $Pb(ac)_2$ was dried under vacuum at 110 °C for 1 h in a 3-neck round-bottom flask. The resultant solution contained no discoloration. This solution was quickly heated to 125–135 °C under moderate N_2 flow, and 2 mL of a 1:1 mixture of 1 M TOPSe/TOP was rapidly injected. The temperature remained constant, and the particles were grown for 5 min. This procedure only forms radially symmetric 3–4 nm particles.

Method C. Synthesis of PbSe Multipods in Acetic Acid Treated Squalene. A solution of 4 mL of squalene, 2 mmol acetic acid, and 3 mmol water was heated to 110 °C under N_2 for 3 h in a round-bottom flask. The resultant viscous yellow solution was dried under vacuum at 110 °C for 3 h to remove excess acetic acid; multiple iterations of this process were performed for some experiments as discussed below. For multiple reactions between squalene and acetic acid, the squalene was dried thoroughly and analyzed by FTIR for purity. This treated squalene was then added to 1 mL of TOP, 3 mmol oleic acid, and 1 mmol $Pb(ac)_2$ in a 3-neck round-bottom flask. The mixture was dried at 110 °C under vacuum for 1 h to remove water. The resultant mixture had a deep yellow discoloration. The temperature was raised quickly to 125–135 °C under N_2 and 2 mL of a solution of 1:1 1 M TOPSe/TOP was rapidly injected into the solution. Aliquots were taken out at 30, 60, and 120 s after initial injection and quenched in hexane. These aliquots were precipitated in hexane with the addition of ethanol and investigated *via* TEM microscopy to elucidate growth mechanics.

Acknowledgment. This work was supported by the University of Illinois at Chicago and the U.S. Air Force Surgeon General's Office of Modernization under Contract FA7014-07-C-0047. We thank Justin C. Johnson for helpful discussions and Luke Hanley for helpful discussions and assistance with several experiments and characterizations performed in this study.

Supporting Information Available: Additional methods of synthesis, FTIR and NMR spectra of acid-treated squalene, additional TEM micrographs of control samples, Pb and Se XPS data, statistical analysis of low aspect ratio PbSe rod structure, and emission data. This material is available free of charge *via* the Internet at http://pubs.acs.org.

REFERENCES AND NOTES

1. Brus, L. E. Electron–Electron and Electron–Hole Interactions in Small Semiconductor Crystallites–The Size Dependence of the Lowest Excited Electronic State. *J. Chem. Phys.* **1984**, *80*, 4403–4409.
2. Murray, C. B.; Norris, D. J.; Bawendi, M. G. Synthesis and Characterization of Nearly Monodisperse CdE (E = S, Se, Te) Semiconductor Nanocrystallites. *J. Am. Chem. Soc.* **1993**, *115*, 8706–8715.
3. Michalet, X.; Pinaud, F. F.; Bentolila, L. A.; Tsay, J. M.; Doose, S.; Li, J. J.; Sundaresan, G.; Wu, A. M.; Gambhir, S. S.; Weiss, S. Quantum Dots for Live Cells, *In Vivo* Imaging, and Diagnostics. *Science* **2005**, *307*, 538–544.
4. Peng, X. G.; Manna, L.; Yang, W. D.; Wickham, J.; Scher, E.; Kadavanich, A.; Alivisatos, A. P. Shape Control of CdSe Nanocrystals. *Nature* **2000**, *404*, 59–61.
5. Asunskis, D. J.; Bolotin, I. L.; Hanley, L. Nonlinear Optical Properties of PbS Nanocrystals Grown in Polymer Solutions. *J. Phys. Chem. C* **2008**, *112*, 9555–9558.
6. Hu, J. T.; Li, L. S.; Yang, W. D.; Manna, L.; Wang, L. W.; Alivisatos, A. P. Linearly Polarized Emission from Colloidal Semiconductor Quantum Rods. *Science* **2001**, *292*, 2060–2063.
7. Katz, D.; Wizansky, T.; Millo, O.; Rothenberg, E.; Mokari, T.; Banin, U. Size-Dependent Tunneling and Optical Spectroscopy of CdSe Quantum Rods. *Phys. Rev. Lett.* **2002**, *89*, 086801.
8. Millo, O.; Katz, D.; Steiner, D.; Rothenberg, E.; Mokari, T.; Kazes, M.; Banin, U. Charging and Quantum Size Effects in Tunneling and Optical Spectroscopy of CdSe Nanorods. *Nanotechnology.* **2004**, *15*, R1–R6.
9. Rothenberg, E.; Mokari, T.; Kazes, M.; Banin, U.; Katz, D.; Steiner, D.; Millo, O. Electronic Level Structure and Single Electron Tunneling Effects in CdSe Quantum Rods. *Israel J. Chem.* **2004**, *44*, 391–400.
10. Kazes, M.; Lewis, D. Y.; Banin, U. Method for Preparation of Semiconductor Quantum-Rod Lasers in a Cylindrical Microcavity. *Adv. Funct. Mater.* **2004**, *14*, 957–962.
11. Kazes, M.; Lewis, D. Y.; Ebenstein, Y.; Mokari, T.; Banin, U. Lasing from Semiconductor Quantum Rods in a Cylindrical Microcavity. *Adv. Mater.* **2002**, *14*, 317–321.
12. Costi, R.; Saunders, A. E.; Elmalem, E.; Salant, A.; Banin, U. Visible Light-Induced Charge Retention and Photocatalysis with Hybrid CdSe–Au Nanodumbbells. *Nano Lett.* **2008**, *8*, 637–641.
13. Costi, R.; Cohen, G.; Salant, A.; Rabani, E.; Banin, U. Electrostatic Force Microscopy Study of Single Au–CdSe Hybrid Nanodumbbells: Evidence for Light-Induced Charge Separation. *Nano Lett.* **2009**, *9*, 2031–2039.
14. Elmalem, E.; Saunders, A. E.; Costi, R.; Salant, A.; Banin, U. Growth of Photocatalytic CdSe–Pt Nanorods and Nanonets. *Adv. Mater.* **2008**, *20*, 4312–4317.
15. Huynh, W. U.; Dittmer, J. J.; Alivisatos, A. P. Hybrid Nanorod–Polymer Solar Cells. *Science* **2002**, *295*, 2425–2427.
16. Huynh, W. U.; Dittmer, J. J.; Libby, W. C.; Whiting, G. L.; Alivisatos, A. P. Controlling the Morphology of Nanocrystal–Polymer Composites for Solar Cells. *Adv. Funct. Mater.* **2003**, *13*, 73–79.
17. Huynh, W. U.; Dittmer, J. J.; Teclemariam, N.; Milliron, D. J.; Alivisatos, A. P.; Barnham, K. W. J. Charge Transport in Hybrid Nanorod–Polymer Composite Photovoltaic Cells. *Phys. Rev. B* **2003**, *67*, 12.
18. Dukovic, G.; Merkle, M. G.; Nelson, J. H.; Hughes, S. M.; Alivisatos, A. P. Photodeposition of Pt on Colloidal CdS and CdSe/CdS Semiconductor Nanostructures. *Adv. Mater.* **2008**, *20*, 4306–4311.
19. Amirav, L.; Alivisatos, A. P. Photocatalytic Hydrogen Production with Tunable Nanorod Heterostructures. *J. Phys. Chem. Lett.* **2010**, *1*, 1051–1054.
20. Pietryga, J. M.; Schaller, R. D.; Werder, D.; Stewart, M. H.; Klimov, V. I.; Hollingsworth, J. A. Pushing the Band Gap Envelope: Mid-infrared Emitting Colloidal PbSe Quantum Dots. *J. Am. Chem. Soc.* **2004**, *126*, 11752–11753.
21. Steckel, J. S.; Coe-Sullivan, S.; Bulovic, V.; Bawendi, M. G. 1.3 to 1.55 μm Tunable Electroluminescence from PbSe Quantum Dots Embedded within an Organic Device. *Adv. Mater.* **2003**, *15*, 1862–1866.
22. Hull, K. L.; Grebinski, J. W.; Kosel, T. H.; Kuno, M. Induced Branching in Confined PbSe Nanowires. *Chem. Mater.* **2005**, *17*, 4416–4425.

23. Yong, K. T.; Sahoo, Y.; Choudhury, K. R.; Swihart, M. T.; Minter, J. R.; Prasad, P. N. Shape Control of PbSe Nanocrystals Using Noble Metal Seed Particles. *Nano Lett.* **2006**, *6*, 709–714.
24. Shi, W. L.; Sahoo, Y.; Zeng, H.; Ding, Y.; Swihart, M. T.; Prasad, P. N. Anisotropic Growth of PbSe Nanocrystals on Au-Fe_3O_4 Hybrid Nanoparticles. *Adv. Mater.* **2006**, *18*, 1889–1894.
25. Luther, J. M.; Zheng, H. M.; Sadtler, B.; Alivisatos, A. P. Synthesis of PbS Nanorods and Other Ionic Nanocrystals of Complex Morphology by Sequential Cation Exchange Reactions. *J. Am. Chem. Soc.* **2009**, *131*, 16851–16857.
26. Lifshitz, E.; Bashouti, M.; Kloper, V.; Kigel, A.; Eisen, M. S.; Berger, S. Synthesis and Characterization of PbSe Quantum Wires, Multipods, Quantum Rods, and Cubes. *Nano Lett.* **2003**, *3*, 857–862.
27. Banfield, J. F.; Welch, S. A.; Zhang, H. Z.; Ebert, T. T.; Penn, R. L. Aggregation-based Crystal Growth and Microstructure Development in Natural Iron Oxyhydroxide Biomineralization Products. *Science* **2000**, *289*, 751–754.
28. Pacholski, C.; Kornowski, A.; Weller, H. Self-Assembly of ZnO: From Nanodots to Nanorods. *Angew. Chem., Int. Ed.* **2002**, *41*, 1188–1191.
29. Cho, K. S.; Talapin, D. V.; Gaschler, W.; Murray, C. B. Designing PbSe Nanowires and Nanorings Through Oriented Attachment of Nanoparticles. *J. Am. Chem. Soc.* **2005**, *127*, 7140–7147.
30. Koh, W. K.; Bartnik, A. C.; Wise, F. W.; Murray, C. B. Synthesis of Monodisperse PbSe Nanorods: A Case for Oriented Attachment. *J. Am. Chem. Soc.* **2010**, *132*, 3909–3913.
31. Mokari, T.; Rothenberg, E.; Popov, I.; Costi, R.; Banin, U. Selective Growth of Metal Tips onto Semiconductor Quantum Rods and Tetrapods. *Science* **2004**, *304*, 1787–1790.
32. Halpert, J. E.; Porter, V. J.; Zimmer, J. P.; Bawendi, M. G. Synthesis of CdSe/CdTe nanobarbells. *J. Am. Chem. Soc.* **2006**, *128*, 12590–12591.
33. Bolotin, I. L.; Asunskis, D. J.; Jawaid, A. M.; Liu, Y. M.; Snee, P. T.; Hanley, L. Effects of Surface Chemistry on Nonlinear Absorption, Scattering, and Refraction of PbSe and PbS Nanocrystals. *J. Phys. Chem. C* **2010**, *114*, 16257–16262.
34. Harding, W. W.; Simpson, D. S.; Jacobs, H.; McLean, S.; Reynolds, W. F. A New Squalene-derived Epoxy tri-THF diol from *Spathelia glabrescens*. *Tetrahedron Lett.* **2001**, *42*, 7379–7381.
35. Heiba, E. I.; Dessau, R. M.; Rodewald, P. G. Oxidation by Metal Salts. X. One-Step Synthesis of γ-Lactones from Olefins. *J. Am. Chem. Soc.* **1974**, *96*, 7977–7981.
36. *Spectral Database for Organic Compounds*; National Institute of Advanced Industrial Science and Technology (AIST): Japan, 2010.
37. Lee, S. M.; Jun, Y. W.; Cho, S. N.; Cheon, J. Single-Crystalline Star-Shaped Nanocrystals and Their Evolution: Programming the Geometry of Nano-building Blocks. *J. Am. Chem. Soc.* **2002**, *124*, 11244–11245.
38. Kigel, A.; Brumer, M.; Sashchiuk, A.; Amirav, L.; Lifshitz, E. PbSe/$PbSe_xS_{1-x}$ Core-Alloyed Shell Nanocrystals. *Mater. Sci. Eng., C* **2005**, *25*, 604–608.
39. Dai, Q. Q.; Wang, Y. N.; Zhang, Y.; Li, X. B.; Li, R. W.; Zou, B.; Seo, J.; Wang, Y. D.; Liu, M. H.; Yu, W. W. Stability Study of PbSe Semiconductor Nanocrystals over Concentration, Size, Atmosphere, and Light Exposure. *Langmuir* **2009**, *25*, 12320–12324.